



Influence of carbon content on microstructure and mechanical properties of 1000 MPa deposited metal by gas metal arc welding

Tong-bang An^{1,2} · Jin-shan Wei¹ · Lin Zhao¹ · Ji-guo Shan² · Zhi-ling Tian¹

Received: 19 July 2018 / Revised: 8 November 2018 / Accepted: 22 November 2018 / Published online: 10 May 2019
© China Iron and Steel Research Institute Group 2019

Abstract

The effects of carbon content (0.078–0.100 wt.%) on the microstructure and properties of 1000 MPa grade deposited metal produced by gas metal arc welding have been investigated. Experimental results show that the microstructure of the deposited metal was mainly composed of martensite, bainite and retained austenite. With increasing carbon content, the proportion of martensite increased, and the amount of bainite was reduced. High carbon content is beneficial to strength, but harmful to impact toughness, and thus, carbon reductions lead to the increase in impact toughness. When the carbon content was 0.100 wt.%, the lowest Charpy absorbed energy of 47 J at $-40\text{ }^{\circ}\text{C}$ for the deposited metal was achieved, the highest yield strength of 1038 MPa was attained, and the yield-to-tensile ratio was more than 0.88, while the highest Charpy absorbed energy of 55.7 J at $-40\text{ }^{\circ}\text{C}$ and the lowest yield strength of 915 MPa were obtained when the deposited metal contains 0.078 wt.% C, and the yield-to-tensile ratio was less than 0.85. It is concluded that bainite fraction and fine effective grain size were the dominant factors to achieve good comprehensive mechanical properties (the required strength and an acceptable toughness) of deposited metals with various carbon contents.

Keywords 1000 MPa grade deposited metal · Carbon content · Microstructure · Strength · Gas metal arc welding · Impact toughness

1 Introduction

In recent years, high- and ultra-high-strength steels have been developed and used in lightweight constructions (such as the structural components of mobile equipment) to reduce weight and fabrication costs and enhance the performance [1]. Welding of steels with yield strength of more than 900 MPa is particularly challenging because of the toughness requirements for the weld metal, which call for welding consumables of high strength and good toughness [2]. In many occasions, there is an engineering requirement that only a weld metal with matching or overmatching strength can be used in the joining.

Weld metals have been produced by a variety of welding methods to obtain yield strength up to or above 1000 MPa, but its toughness generally needs to be carefully handled. Proper microstructure is the key to achieve optimal combination of strength and toughness, and the final microstructure depends on the chemical composition and cooling rate [3]. Some studies on the influence of heat input and alloying elements on the mechanical properties of high-strength weld metal have been conducted in the past few decades, and results indicated that the optimum range of cooling time from 800 to 500 $^{\circ}\text{C}$ is about 3–13 s [4–7]. In this range, a fine mixed structure of bainite and martensite was obtained, which predominantly contributed to good strength and toughness.

The composition of deposited metal produced by gas metal arc welding (GMAW) depends on the welding wire and shielding gas. The cooling rate of weld metal is controlled by a combination of heat input and extraction. Controlling the microstructure of weld metal and raising the welding productivity are critical factors for the development of weld metal of high-strength steel to obtain ideal mechanical properties

✉ Tong-bang An
antongb@163.com

¹ Central Iron & Steel Research Institute, Beijing 100081, China

² Department of Mechanical Engineering, Tsinghua University, Beijing 100084, China

and to reduce production costs [8]. The microstructures of these weld metals are generally a mixture of ferrite, bainite, martensite and retained austenite [6]. However, the microstructure suitable for weld metals with yield strength over 690 MPa has been the subject of much discussion, and these results indicated that microstructures can be classified into three groups: acicular ferrite with small amounts of bainite [6, 9], a mixture of acicular ferrite and martensite [6, 10, 11] and a mixture of bainite and martensite [12–15]. Lord [16] developed a series of welding wires with yield strength over 800 MPa, and the main structure is the mixture of bainite and martensite. Previous study has shown that carbon could stabilize austenite to lower transformation temperatures of high-strength weld metal and lead to higher martensite constituent in microstructure [17].

In present study, three deposited metals with carbon contents of 0.078, 0.089 and 0.100 wt.% were produced by GMAW to elucidate the effect of variations in carbon content on the microstructure and mechanical properties of 1000 MPa high-strength deposited metal, and Hall–Petch-type analysis on the impact toughness of the lath martensite/bainite in the three deposited metals is made with respect to the packet size and the block size, respectively, to clarify the role played by the packet or block boundaries in determining the impact toughness of the lath martensite/bainite.

2 Experimental materials and procedures

High-strength low-alloy (HSLA) steel with minimum yield strength of 960 MPa was prepared in dimensions of 500 mm × 150 mm × 20 mm as base material with a

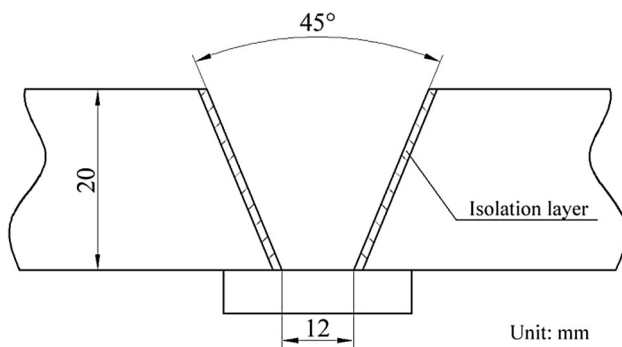


Fig. 1 Schematic diagram of weld joint

V-type groove (Fig. 1). The chemical composition of the base metal is summarized in Table 1. The welding was conducted using the GMAW process. Before welding, plates were ground and grooved. Three kinds of solid welding wires with diameter of 1.2 mm were used as filler wires. The compositions of deposited metal are shown in Table 2. All the deposited metals were welded with welding current of 280 A, welding voltage of 28 V, welding speed of 36 cm/min, heat input of 13 kJ/cm and interpass temperature of 100–110 °C. Shielding gas was 80 vol.% Ar + 20 vol.% CO₂ with a steady flow rate of 20 L/min.

Tensile specimens were machined longitudinally from the center of the deposited metals with a specimen diameter of 10 mm and a gauge length of 60 mm. For Charpy impact test, transverse specimens were machined in dimensions of 55 mm × 10 mm × 10 mm, and the V-type groove was notched in the center of the deposited metal, perpendicular to the welding direction. The impact tests were conducted at room temperature (RT) and –40 °C, and three specimens were tested at each temperature. Observation of transversal sections was conducted on an optical microscope (OM, Leica MEF4 M) and a scanning electron microscope (SEM, Hitachi S4300). The deposited metal was etched with 3 vol.% nital to reveal microstructure. However, it is difficult to distinguish bainite and martensite plates since their dimensions are less than the wavelength of ray in even conventional SEM; thus, LePera solution was applied to reveal martensite as brown and bainite as mazarine [18]. Transmission electron microscopy (TEM) observation was carried out on an H-800 microscope operating at 176 kV for more microstructure details. The volume fraction of retained austenite was measured by X-ray diffraction. The prior austenite grain size, packet size on the fracture surfaces of impact specimens and block width were statistically determined by metallographic microscopy, SEM and electron backscatter

Table 2 Chemical compositions of deposited metals (wt.%)

Metal	C	Si	Mn	Ni	Cr	Mo	Ti	Fe
No. 1	0.078	0.46	1.53	2.32	0.56	0.87	0.039	Balance
No. 2	0.089	0.47	1.46	2.38	0.56	0.86	0.045	Balance
No. 3	0.100	0.46	1.49	2.37	0.57	0.87	0.041	Balance

Table 1 Chemical composition of base metal (wt.%)

C	Si	Mn	S	P	Ni + Cr + Mo	Cu	Ti + Nb	Fe
0.14	0.41	1.18	0.0016	0.0081	0.8986	0.015	0.025	Balance

diffraction (EBSD), respectively. EBSD analysis was performed on $\phi 3$ mm jet electro-polished disks with thickness of 80–100 μm via an FEI Quanta 650 field emission gun scanning electron microscope (FEGSEM) equipped with the HKL technology EBSD system.

3 Results and discussion

3.1 Evolution of microstructure

As we know, property of weld metal is mainly determined by the microstructure of low-alloy steel welds, and the microstructure of welds is heavily dependent on chemical composition. In particular, the weld joint was usually composed of different regions with non-homogenous microstructure. The last bead which has not been re-heated is analyzed considering thermal cycle effect of the multi-run and multilayer welds. Optical microstructure of deposited metals with different carbon contents is shown in Fig. 2. The deposited metal in this investigation is composed of martensite and bainite. Due to the effect of carbon on phase transformation mechanism, more martensite can be obtained as carbon content increases.

For deposited metal No. 1, the microstructure is a fine mixture of lath martensite and interlocked bainite with different orientations. As carbon content of deposited metals increases, bainite decreases and martensite gradually becomes the dominant microstructural component (deposited metals No. 2 and No. 3). Deposited metal No. 3 exhibits significantly different microstructures compared with deposited metals No. 1 and No. 2. Its microstructure is mainly composed of martensite and a small amount of bainite with different orientations. In this process, the martensite lath morphology becomes vague.

Figure 3 shows the TEM micrographs of deposited metals with different carbon contents. With increasing carbon content, the martensite lath morphology changes from intertexture to parallel, and the average width of bainite/martensite lath decreases gradually. For deposited metal No. 1, the average width of bainite/martensite lath is about 0.5–1.0 μm and bainite and martensite are interlocked (Fig. 3a). For deposited metal No. 2, the width of bainite/martensite plates is about 0.5 μm and the intertexture morphology is not obvious (Fig. 3b). For deposited metal No. 3, the laths are approximately parallel to each other and their average width is below 0.5 μm (Fig. 3c). It can be regarded as low carbon martensite because its morphology exhibits a rather high dislocation density. Retained austenite is found between the bainite/martensite laths (Fig. 3d), which is beneficial to toughness promotion, as demonstrated in Refs. [19, 20]. Quantitative measurements were made by X-ray diffraction. The fraction of

retained austenite in deposited metals with increased carbon content is 2.49, 2.58 and 2.60 vol.%, respectively.

LePera reagent was applied to distinguish martensite and bainite of deposited metals and made martensite colored brown and bainite colored mazarine. As carbon

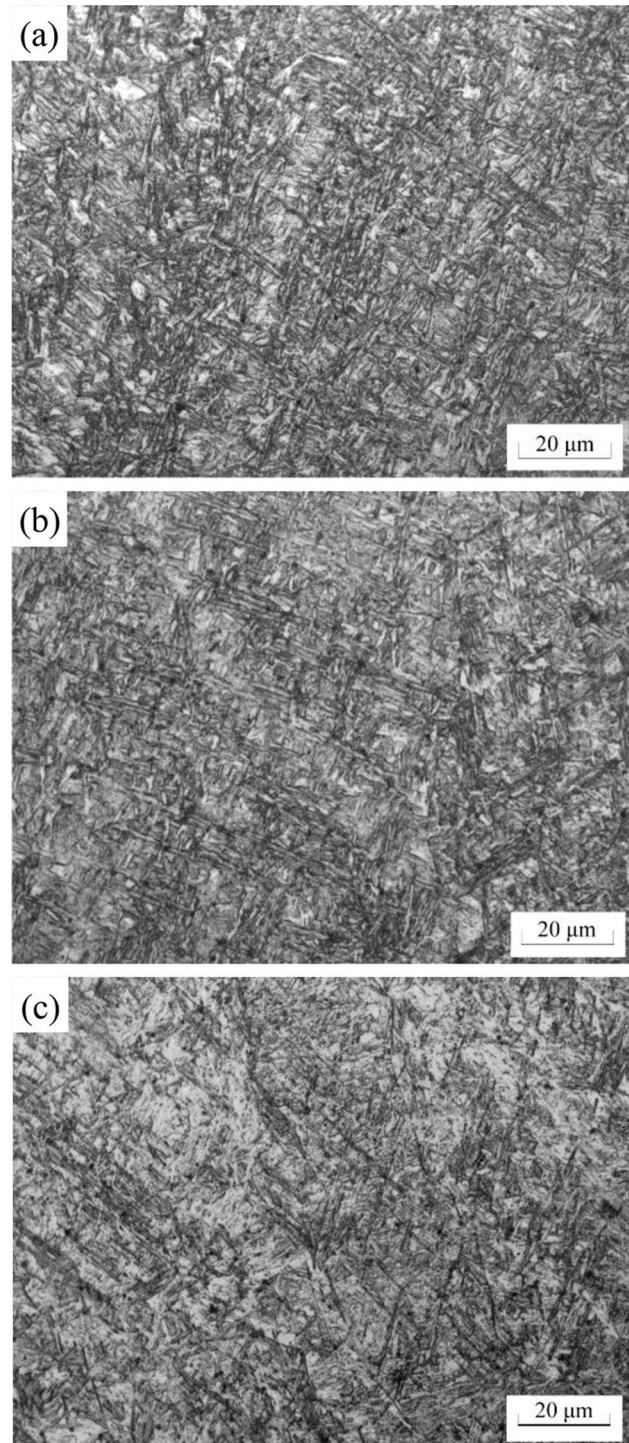


Fig. 2 OM images of as-deposited top beads with different carbon contents. **a** 0.078 wt.%; **b** 0.089 wt.%; **c** 0.100 wt.%

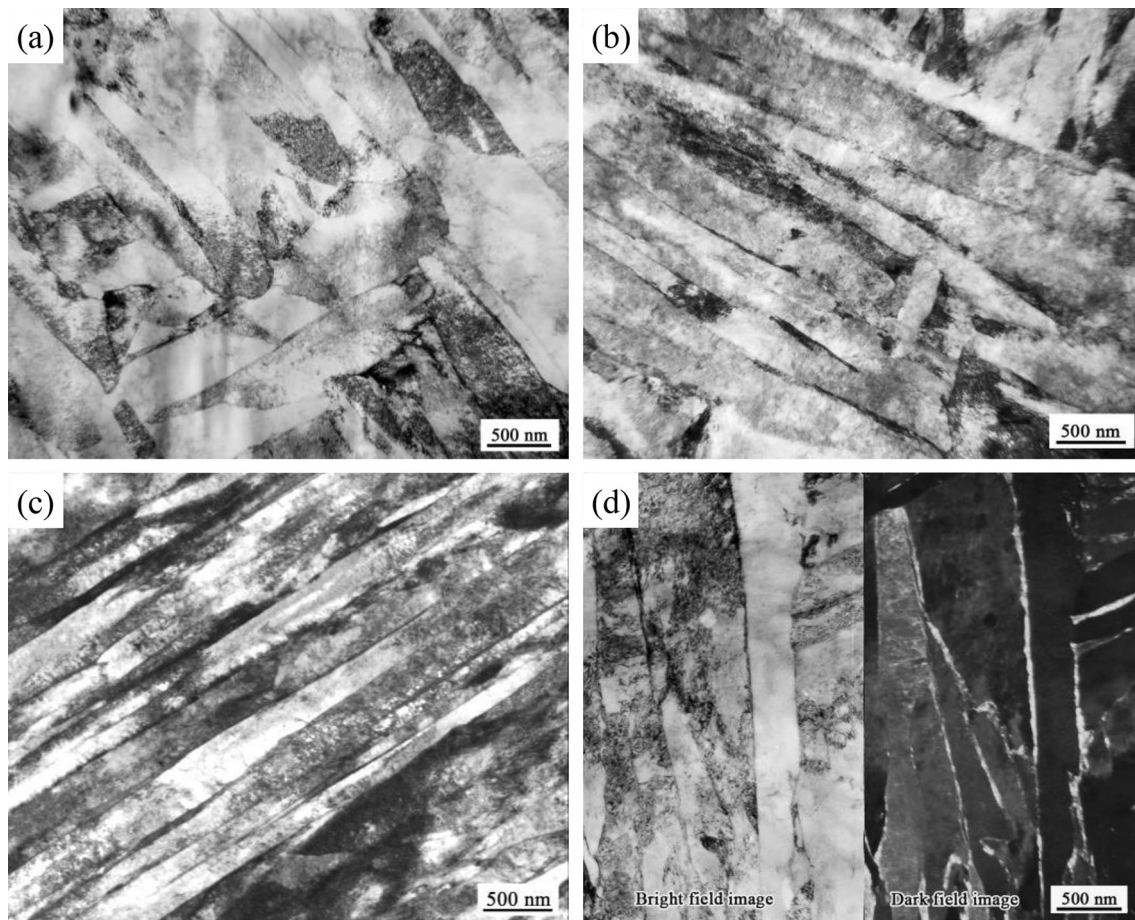


Fig. 3 TEM images of martensite/bainite lath structure of deposited metal with different carbon contents. **a** 0.078 wt.%; **b** 0.089 wt.%; **c** 0.100 wt.%; **d** bright-/dark-field image of retained austenite

content decreases, the lath bainites are interlocked, and the amount of bainite is significantly increased, as shown in Fig. 4. This distribution of lath bainite would refine the microstructure, which could be verified as the microstructure in Fig. 4 is refined to some extent. The fractions of martensite calculated by Lepera tint etching and quantitative metallography method are 69.6, 76.2 and 80.3 vol.% in deposited metals No. 1, No. 2 and No. 3, respectively. The content of bainite decreases correspondingly as the carbon content increases.

3.2 Effect of microstructure on strength and toughness

As indicated by above analysis, the microstructure of deposited metal is a mixture of martensite and bainite. The fraction of martensite and the dislocation density increase simultaneously in deposited metal as carbon content increases. It is well known that the mechanical property of deposited metal depends on the microstructure, which is heavily dependent on chemical composition. The relation

between the mechanical property and carbon content of deposited metal is shown in Fig. 5.

In Fig. 5, the results indicate that tensile strength (R_m) and yield strength ($R_{p0.2}$) increase gradually with increasing carbon content, and elongation after fracture (A) and percentage reduction of area (Z) show no obvious change. However, the impact energy is significantly changed. With increasing carbon content, the toughness of deposited metals decreases. As widely known, high carbon content is beneficial to strength, but harmful to impact toughness, and carbon reductions lead to enhanced impact toughness. When the carbon content is 0.100 wt.%, the fraction of bainite is 19.7 vol.%, and the lowest Charpy absorbed energy of 47 J at -40 °C is achieved, and the highest yield strength of 1038 MPa is attained, and the yield-to-tensile ratio is above 0.88. This is due to two factors: The gradual increase in strength caused by carbon addition could contribute to increasing the proportion of martensite, and the plastic constraint effect enhances the strength of bainite [21]. In comparison, the highest Charpy absorbed energy of 55.7 J at -40 °C and the lowest yield strength

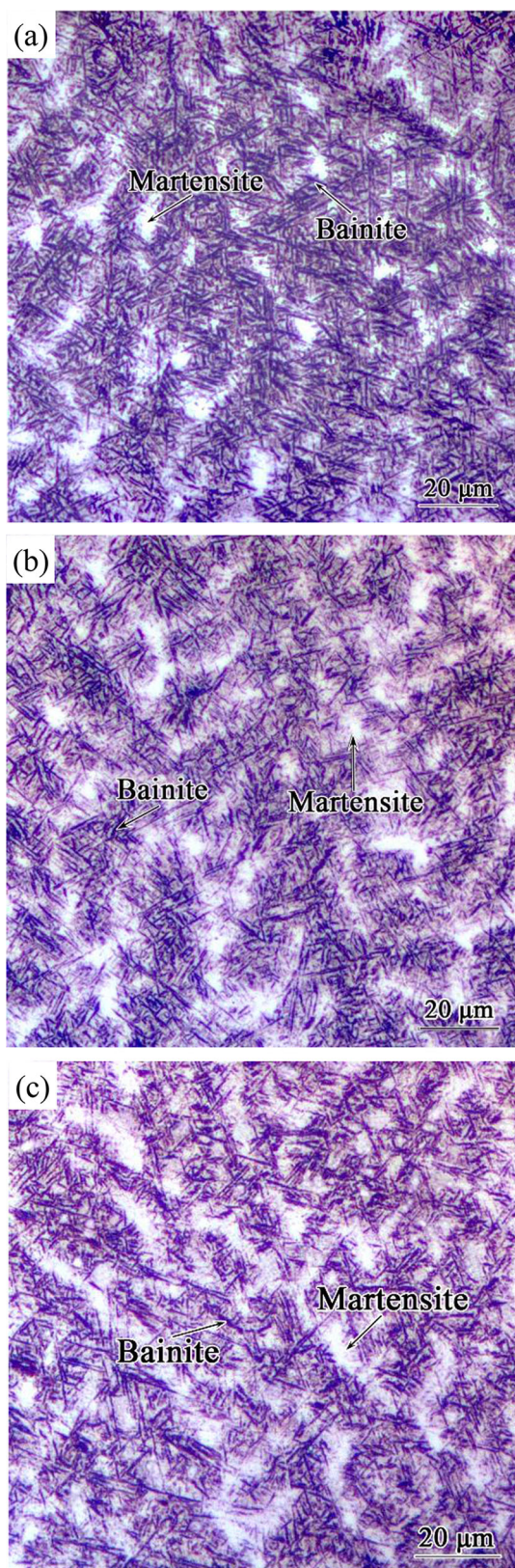


Fig. 4 Color OM images of as-deposited top beads with different carbon contents. **a** 0.078 wt.%; **b** 0.089 wt.%; **c** 0.100 wt.%

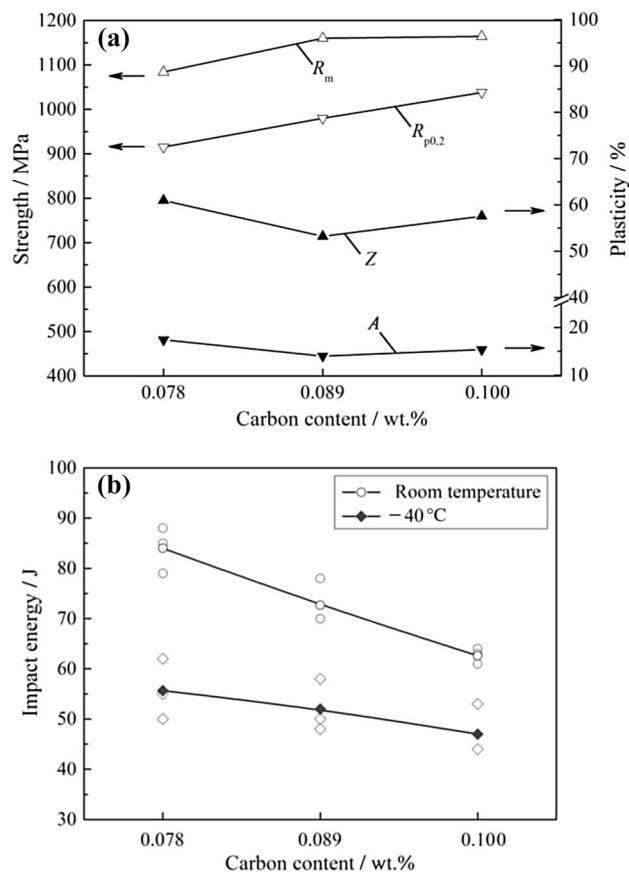


Fig. 5 Tensile property **(a)** and toughness **(b)** of deposited metals

of 915 MPa are obtained when the deposited metal contains 0.078 wt.% C. In this case, the fraction of bainite is 30.4 vol.%, and the yield-to-tensile ratio is less than 0.85.

In the mixed structure of martensite/bainite, the bainite laths formed within a prior austenite grain cut the grain into several packets and further subdivide it into blocks during the phase transformation process [22]. Orientation maps of the martensite/bainite block substructure in the deposited metal were acquired by EBSD, which are shown in Fig. 6. The high angle boundaries ($> 15^\circ$) are indicated by black lines, and the grain with high angle boundaries in martensite/bainite steel is known as a block composed of many laths with the same crystal orientation. Table 3 shows that the prior austenite grain size (columnar grain, around 40 μm) is almost the same in deposited metals with different carbon contents, while the sizes of packet and block of deposited metals increase with increasing carbon content. Since both the block and packet boundaries are high angle boundaries, they are considered as effective grain sizes because propagating cracks are frequently deflected at high angle boundaries. All tests show that the size of packet and block changes obviously; the smaller effective grain size, the larger grain boundary surface, which increases the toughness significantly.

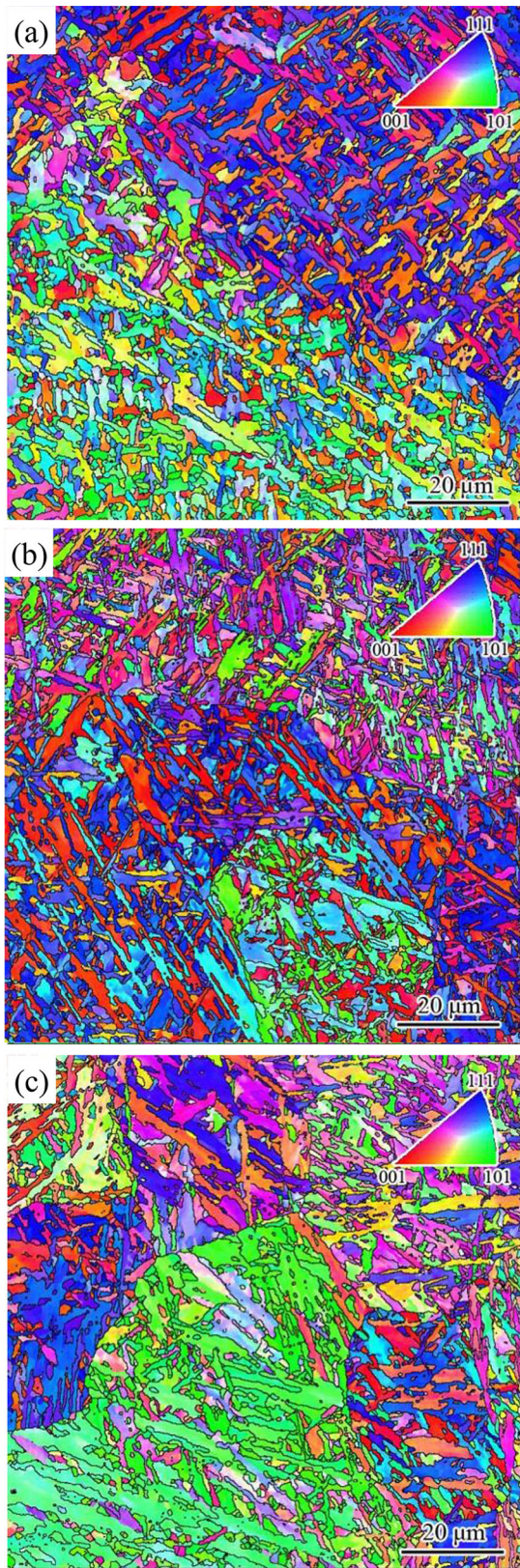


Fig. 6 EBSD orientation maps of martensite/bainite block substructure in deposited metal and inverse pole figures (insets) with different carbon contents. **a** 0.078 wt.%; **b** 0.089 wt.%; **c** 0.100 wt.%

Table 3 Microstructural sizes of deposited metals with mixed structure of martensite and bainite

Carbon content/wt.%	Prior austenite grain size/ μm	Packet size/ μm	Block size/ μm
0.078	39.84	11.55	1.59
0.089	39.76	12.54	1.68
0.100	40.36	13.36	1.73

The opinions on the substructure for controlling toughness are different. Some researchers believe that the packet size should be the effective grain size for controlling cleavage fracture [23, 24], and others think that the block size should be the effective grain size [25, 26]. However, it is generally acknowledged that the misorientations of the packet and block boundaries are high angles that are well determined by the orientation relationship (e.g., Kurdjumov–Sachs, K–S), and the boundaries are expected to act as barriers of the moving dislocations during deformation of the lath bainite/martensite structure and thus to improve toughness, while the misorientations across lath boundaries are low angles that vary within a few degrees [27]. As shown in Table 3, the block width is much smaller than the packet size, indicating that the high angle boundaries in the structure are dominated by the block boundaries.

The analysis of toughness controlled by substructure is conducted based on the fact that the variation of packet and block size can influence impact toughness. Figure 7 shows the Hall–Petch-type plots of Charpy impact energy as functions of packet size and block width at room temperature and $-40\text{ }^{\circ}\text{C}$ for the deposited metals with different carbon contents. A linear regression of the plots is given, indicating that the Hall–Petch slopes of Charpy impact energy versus packet size and Charpy impact energy versus block width are 11 and 144 at room temperature, 4.83 and 60 at $-40\text{ }^{\circ}\text{C}$, respectively. Based on the data above, it can be seen that the effect of block width on Charpy impact energy is greater than that of packet size, although both packet size and block width are generally regarded as effective grain sizes due to the high angle boundaries of packets and blocks. Hence, the block width is the dominated microstructural unit controlling toughness.

4 Conclusions

1. The microstructure of deposited metal was mainly composed of lath bainite and martensite. With increasing the carbon content, the proportion of martensite increases, while that of bainite decreases.
2. As the carbon content of deposited metal increased from 0.078 to 0.100 wt.%, its yield strength increased

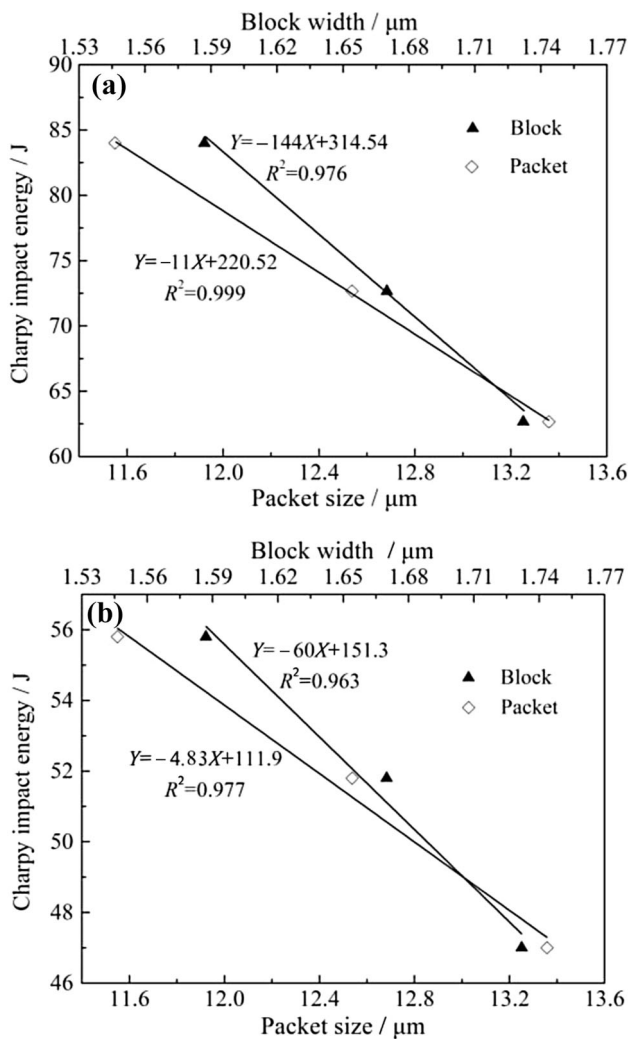


Fig. 7 Relationship of Charpy impact energy versus packet size and block width. **a** Room temperature; **b** - 40 °C. R^2 —Coefficient of determination

from 915.2 to 1038.0 MPa, and Charpy impact energy decreased from 55.7 to 47.0 J.

- The packet size and block width decreased as the proportion of bainite increased. The influence of block width on Charpy impact energy was much greater than that of packet size. The block was a smaller substructure, and the block width can be regarded as the microstructural factor for controlling toughness. The effective grain size decreases with the increasing bainite content. Bainite fraction and fine effective grain size were the dominant factors to achieve good mechanical properties of the deposited metal.

Acknowledgements This work was supported by National Key R&D Plan of China (2017YFB0305100 and 2017YFB0305105).

References

- [1] E.A. Gyasi, P. Kah, H. Wu, M.A. Kesse, *Int. J. Adv. Manuf. Technol.* 93 (2017) 1139–1155.
- [2] J.S. Seo, C.H. Lee, H.J. Kim, *ISIJ Int.* 53 (2013) 279–285.
- [3] Y. Kang, S. Jeong, J.H. Kang, C. Lee, *Metall. Mater. Trans. A* 47 (2016) 2842–2854.
- [4] E. Keehan, J. Zachrisson, L. Karlsson, *Sci. Technol. Weld. Join.* 15 (2010) 233–238.
- [5] W.S. Du, Y. Peng, H.J. Xiao, C.H. He, Z.L. Tian, *Mater. Sci. Forum* 638–642 (2010) 3441–3446.
- [6] T.L. Zhang, Z.X. Li, S.M. Ma, S. Kou, H.Y. Jing, *Sci. Technol. Weld. Join.* 21 (2016) 186–193.
- [7] P. Haslberger, S. Holly, W. Ernst, R. Schnitzer, *J. Mater. Sci.* 53 (2018) 6968–6979.
- [8] M. Gouda, M. Takahashi, K. Ikeuchi, *Sci. Technol. Weld. Join.* 10 (2005) 369–377.
- [9] Z. Yang, T. Debroy, *Metall. Mater. Trans. A* 30 (1999) 483–493.
- [10] J.E. Ramirez, S. Liu, D.L. Olson, *Mater. Sci. Eng. A* 216 (1996) 91–103.
- [11] D.A. Fleming, A.Q. Bracarense, S. Liu, D.L. Olson, *Weld. J.* 75 (1996) 171–183.
- [12] N.A. Fleck, O. Grong, G.R. Edwards, D.K. Matlock, *Weld. J.* 65 (1986) 113–121.
- [13] P. Haslberger, W. Ernst, R. Schnitzer, *Sci. Technol. Weld. Join.* 22 (2017) 336–342.
- [14] K. Sampath, R.S. Green, D.A. Civis, B.E. Williams, P.J. Konkol, *Weld. J.* 74 (1995) 69–76.
- [15] Y. Peng, X.N. Peng, X.M. Zhang, Z.L. Tian, T. Wang, *J. Iron Steel Res. Int.* 21 (2014) 539–544.
- [16] M. Lord, *Design and modelling of ultra-high strength steel weld deposits*, University of Cambridge, London, UK, 1999.
- [17] E. Keehan, L. Karlsson, H.O. Andrén, H.K.D.H. Bhadeshia, *Sci. Technol. Weld. Join.* 11 (2006) 19–24.
- [18] E. Girault, P. Jacques, Ph. Harlet, K. Mols, J. Van Humbeeck, E. Aernoudt, F. Delannay, *Mater. Charact.* 40 (1998) 111–118.
- [19] L.C. Chang, H.K.D.H. Bhadeshia, *Mater. Sci. Technol.* 11 (1995) 874–882.
- [20] V. Biss, R.L. Cryderman, *Metall. Mater. Trans. B* 2 (1971) 2267–2276.
- [21] C.H. Young, H.K.D.H. Bhadeshia, *Mater. Sci. Technol.* 10 (1994) 209–214.
- [22] C.F. Wang, M.Q. Wang, J. Shi, W.J. Hui, H. Dong, *J. Mater. Sci. Technol.* 23(2007) 659–664.
- [23] Y. Tomita, K. Okabayashi, *Metall. Trans. A* 17 (1986) 1203–1209.
- [24] C.F. Wang, M.Q. Wang, J. Shi, W.J. Hui, H. Dong, *Scripta Mater.* 58 (2008) 492–495.
- [25] J.W. Morris, C. Kinney, K. Pytlewski, Y. Adachi, *Sci. Technol. Adv. Mater.* 14 (2013) 14208.
- [26] Q. Wu, M.A. Zikry, *Int. J. Solids Struct.* 51 (2014) 4345–4356.
- [27] S. Morito, H. Yoshida, T. Maki, X. Huang, *Mater. Sci. Eng. A* 438 (2006) 237–240.